ACS OMEGA

Open Access

http://pubs.acs.org/journal/acsodf

Article

High Conversion of Concentrated Sugars to 5-Hydroxymethylfurfural over a Metal-free Carbon Catalyst: Role of Glucose−Fructose Dimers

Athukoralalage Don K. Deshan, Lalehvash Moghaddam, Luqman Atanda, Hongxia Wang, John P. Bartley, William O.S. Doherty, and Darryn W. Rackemann*

Cite This: *ACS Omega* 2023, 8, 40442−40455

Read Online

ACCESS | Metrics & More | Article Recommendations | Supporting Information

ABSTRACT: To reduce the production cost of chemicals from renewable resources, the feedstock loading must be high and the catalyst must be of low cost and efficient. In this study, at a very short reaction time of 10 min at 125 °C, concentrated sugar solutions (20 wt %, 101 wt % on solvent) were converted to 5-hydroxymethylfurfural (HMF) over a cotton gin trash (CGT)-derived sulfonated carbon catalyst in a 1-butyl-3-methylimidazolium chloride ([BMIM]Cl) and 2-methyltetrahydrofuran (MeTHF) biphasic system. We report, for the first time, that the presence of glucose either as a covalently bonded monomer in sucrose or in a mixture with fructose achieved yields of HMF up to 62 mol % compared to a value of only 39 mol % obtained with fructose on its own. In the concentrated reaction medium, glucose, fructose, and sucrose molecules produce difructose anhydrides, dimers/reversion products, and sucrose isomers. The glucose−fructose dimers formed in sucrose and glucose/fructose reaction systems play a critical role in the transformation of the sugars to a higher-than-expected HMF yield. Thus, a strategy of using cellulosic glucose, where it is partially converted to fructose content and the high sugar concentration sugar mixture is then converted to HMF, should be exploited for future biorefineries.

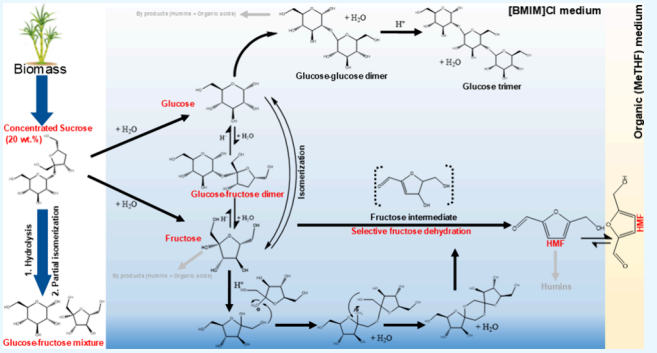

1. INTRODUCTION

The conversion of lignocellulosic biomass to renewable energy is one strategy being investigated to replace fossil fuels and hence reduce greenhouse gas emissions. The European Commission aims that by 2030, 25% of Europe's energy consumption for transportation will be from biofuels and 30% of the fossil-based chemical market will be substituted with biobased products.[1] 5-Hydroxymethylfurfural (HMF) is one of the platform chemicals that can be derived from biomass and serves as an intermediate in biofuels, bioplastics, and biobased chemical production.[2] HMF can be subjected to various chemical reactions such as hydration, oxidation, decarbonylation, hydrogenation, and etherification to form platform chemicals such as levulinic acid, 2,5-furandicarboxylic acids (FDCA), furfuryl alcohol, dimethylfuran, and 5-alckoxymethylfurfural, respectively.[3−6] A wide application of heterogeneous catalysts has successfully been used to convert sugars (including glucose and sucrose) to HMF because of their excellent properties, such as they possess both Lewis and Brønsted acid sites.[7,8] However, issues around the high catalyst cost, HMF selectivity, production efficiency, and catalyst reusability still plague current catalytic systems. Therefore, there is still immense interest in the development of catalysts for this purpose.

In the production of HMF, high sugar loading is favored for commercialization purposes because of the reduced capital investment and operating expenses. In previous studies, mostly Cr and Sn metal salts have been used as catalysts to convert high sugar loading to HMF.[7,8] However, Cr and Sn metal salts create environmental issues due to their toxicity and high acidity.[9,10] Although metal-free biomass-derived sulfonated carbons have gained much attention as catalysts, studies including those by the authors[11,12] have only been limited to sugar concentrations <10 wt %.[13−15] Therefore, studies using biomass-derived sulfonated carbon catalysts to produce high yields of HMF from high sugar concentrations are required to continue the development of effective catalytic systems.

In the conversion of sugars to HMF, the reaction medium is important to increase the HMF yield and facilitate its separation and recovery of the reaction medium. In general,

Received: July 14, 2023
Accepted: September 7, 2023
Published: October 20, 2023

water, organic solvents, and ionic liquids (ILs) are used in the reaction medium for the conversion of sugars to HMF. However, with pure water, the conversion of sugars to HMF is poor.[16] High boiling solvents (e.g., dimethyl sulfoxide (DMSO) and methyl isobutyl ketone (MIBK)) give high HMF yields but require high energy in the distillation process for their recovery.[17] At the same time, HMF losses occur at high operating temperatures because of its degradation.[17] Furthermore, DMSO has high miscibility in other organic solvents, making it challenging to separate HMF by extraction. Ionic liquids have been investigated as efficient reaction media in the conversion of sugars to HMF under mild reaction conditions due to the thermal stability, low vapor pressure, and adjustable chemical properties.[18] Bai et al.[19] have shown that when an IL is used as the reaction medium in the conversion of concentrated glucose solution to HMF, the amount of degradation products formed is reduced, and there is a lower prevalence of catalyst poisoning. To extract HMF from the IL, an organic solvent is added for HMF to partition into it. The work of Abdilla-Santes and team[1] demonstrated that using 2-methyltetrahydrofuran (MeTHF) as the organic phase was effective for HMF extraction (>90% yield).

Herein, we report the conversion of 20 wt % sugar solutions to HMF over a sulfonated carbon catalyst derived from CGT in [BIMIM]Cl and [BMIM]Cl/MeTHF biphasic systems. Through monitoring the reaction products, including reversion products (disaccharides of glucose and fructose) and difructose anhydride (DFA), the impact of glucose in concentrated mixtures with fructose and as a covalently bonded monomer in sucrose on HMF yield was investigated. Furthermore, the reaction pathways for the endothermic dehydration of these sugars were monitored by identifying and characterizing the dimers and sucrose isomers that occur under high sugar concentration conditions that play an undocumented vital role in increasing HMF yield. Whereas DFA is a known intermediate in HMF production from fructose,[20] the glucose−fructose dimer was shown to enhance the catalytic transformation of sugars to HMF in concentrated nonaqueous systems. Glucose addition to concentrated fructose solution (despite the dilution effect) was demonstrated to significantly increase HMF yield when compared to fructose on its own. Therefore, this study provides a strategy for developing a more industrially efficient and sustainable process for HMF synthesis from high sugar concentrations. Glucose can readily be obtained via enzymatic or chemical hydrolysis of lignocellulosic biomass, and then it can be partially isomerized to high fructose content, and the mixture can be transformed to HMF.

2. RESULTS AND DISCUSSION

2.1. Catalyst characterization. The compositional analysis of CGT is shown in Table S1, which shows high glucan and xylan carbohydrate contents and a lower concentration of acid-insoluble materials (lignin-rich) compared to the values reported in literature.[21] The detailed characteristics of the sulfonated carbon catalyst (sulfonated by cholorosulfonic acid) were discussed in our previous work.[22] However, in this work, an in-depth analysis was conducted to elucidate the structure of the HSO_3Cl catalyst. The reaction associated with the chlorosulfonation of CGT derived carbon is as follows, in which "Ar" symbolizes the aromatic group of the carbon catalyst:[22]

$$ArH + 2HSO_3Cl \rightarrow ArSO_2Cl + HCl + H_2SO_4 \quad (1)$$

The effect of chlorosulfonation on carbon structures was compared by the drift-FTIR method. As shown in Figure 1, a

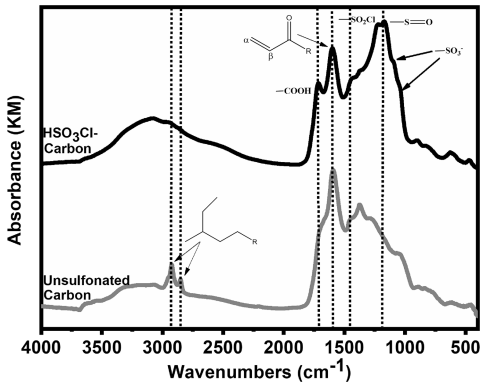

Figure 1. Drift-FTIR spectra of unsulfonated and HSO_3Cl catalyst.

peak is observed at 1192 cm^{-1} corresponding to the −S═O bond, and the peaks at 1026 and 1066 cm^{-1} correspond to the $-SO_3^-$ group.[23] Moreover, a characteristic peak for the $-SO_2Cl$ functional group in the HSO_3Cl catalyst is observed at 1374 cm^{-1}, as reported by Sata et al.[24] The presence of S and Cl groups on the HSO_3Cl catalyst was confirmed with SEM-EDS analysis (Figure S1). The sulfonated catalyst also depicts carbonyl mode peaks at 1720 and 1600 cm^{-1} related to carboxylic acid groups and α,β unsaturated ketone, respectively.[25] Drift-FTIR was also performed on an unsulfonated carbon (Figure 1), and two bands at 2920 and 2850 cm^{-1} corresponding to the nonlinear long-chain aliphatic component were observed.[25,26] However, these nonlinear long chain aliphatic groups have been omitted during chlorosulfonation. The elemental analysis of the HSO_3Cl catalyst indicated the presence of 4.21% S.

The drawback of drift-FTIR is that it does not explain the bond between carbon support and $-SO_3H$ groups.[27] However, X-ray photoelectron spectroscopy (XPS) analysis and ^{13}C CP/MAS NMR are effective methods in identifying covalently bonded $C-SO_3H$ and $-SO_3H$ bonded to the aromatic sites ($Ar-SO_3H$). ^{13}C CP/MAS NMR is particularly useful in identifying $C-SO_3H$ and $Ar-SO_3H$ groups, and the observed spectrum for the HSO_3Cl catalyst is shown in Figure 2. The main peak observed at 126 ppm in the spectrum corresponds to the polyaromatic groups, and the chemical shifts observed at 46, 140, 150, and 177 ppm correspond to the $C-SO_3H$, $Ar-SO_3H$, Ar−OH, and Ar−COOH groups, respectively.[28] XPS analysis of the HSO_3Cl catalyst resulted in two sulfonate groups relating to $-SO_3H$ and $-C-SO_3^-$ in its S 2p high-resolution spectra (Figure S 2d).[29] However, $-SO_3H$ is the primary active site, and the S═O bond in both functional groups acts as a cocatalyst in a less effective manner.[30]

C 1s high-resolution XPS analysis was conducted on the HSO_3Cl catalyst (Figure S2b) and showed five deconvoluted peaks for C−C/C═C, C═O, C−S, COOH, and CO_3^{2-} species.[31,32] Furthermore, the O 1s spectrum in Figure S2c exhibits O−S bonds in sulfonic groups at ∼532.3 eV.[33] Apart from that, the functional groups C−O/C═O, O═C−O, and C−OH were observed at around 530.1−531.6, 532.3−532.8, 533.4−534.1, and 534.4−535.9 eV.[34] As we previously reported, the total acidity of the sulfonated carbon is 5.01 mmol g^{-1}, and the acid site distributions of $-SO_3H/-SO_3^-$, −OH, and −COOH are 2.77, 0.90, and 1.34 mmol g^{-1},

https://doi.org/10.1021/acsomega.3c05060
ACS Omega 2023, 8, 40442−40455

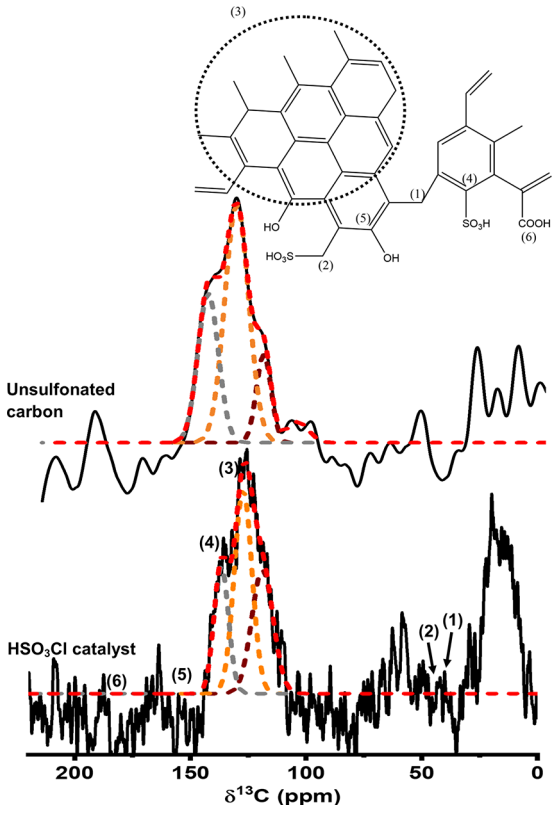

Figure 2. ^{13}C CP/MAS NMR spectra of unsulfonated and HSO_3Cl catalysts with corresponding functional groups.

respectively.[12] The N_2 adsorption−desorption isotherms and nonlocal density functional theory (NLDFT) based pore size distribution spectra of the catalyst exhibited a microporous structure with a type I isotherm with pore diameter distribution in the micropore region (<2 nm) and total specific surface area of 527 m^2 g^{-1} (Figure S3a,b).[35,36] The evaluation of the XRD results for this catalyst (Figure S3c)[29] determined that, contrary to reported results in the literature,[29,30] it is difficult to assign the functional groups using the ϒ peak at ∼24° 2θ, and so the pendant groups (i.e., long-chain aliphatics and functional groups) cannot be present as repeat structures. These pendant groups are likely to be introduced on the edges of the carbon material, as demonstrated in previous studies.[37,38]

2.2. Conversion of Concentrated Sugars to HMF.

Initially, concentrated fructose (20 wt %) was converted in the [BMIM]Cl monophasic system, and the maximum amount of HMF formed was 19.5 mol % at 100 °C in 10 min and increased to 36.3 mol % at 125 °C in 10 min, as shown in Figure 3a and Table 1 entries 1 and 2. Under similar conditions, the HMF yield increased to 37.7 mol % in the biphasic system at 100 °C in 10 min and 39.3 mol % at 125 °C in 10 min. When sucrose was used in the biphasic system, it was hydrolyzed and dehydrated to HMF (55.0 mol %) while forming DFA and reversion products/C6 dimers (16.1 mol %, see Section 2.3 for identification of DFA and C6 dimers) and <1 mol % of formic, acetic, and levulinic acids as byproducts (Table 1 entry 8). A higher HMF yield (58.4 mol %) was obtained with the 50:50 mixture of glucose and fructose with 0.2 mol % fructose and 24.3 mol % glucose unconverted (Table 1 entry 11). So, the amount of converted glucose is slightly more in the glucose/fructose mixture than in sucrose. However, fructose on its own achieved ∼40 mol % yield of HMF, making it less efficient. The predominant path for the dehydration of sugars to HMF is via fructose,[39] so the increase in HMF yield obtained with both sucrose and the glucose/fructose mixture cannot be explained unless there is a dilution effect and/or a significant glucose conversion occurred in these systems that made it possible for these reactions to follow the fructose intermediate pathway to HMF.

The optimum ratio of glucose/fructose for the formation of HMF was studied at 125 °C for 10 min in the [BMIM]Cl/MeTHF biphasic system. As shown in Table 1 entries 9−13 (and Figure 3b and Figure S4), HMF yield increases sharply with fructose addition to glucose to a glucose/fructose weight ratio of 50:50 (58.4 mol %), increases gradually with the fructose addition to a glucose/fructose weight ratio of 10:90 to a value of 61.8 mol %, and then drops sharply with 100% fructose. Therefore, it is inferred that, at a particular glucose/fructose ratio, glucose contributes to the conversion of fructose to HMF. Moreover, the dilution role of glucose in the increase in HMF yield was conducted using 18 wt % of fructose solution, which is the equivalent amount present in the glucose/fructose system of 10:90. A lower HMF yield of 46.2 mol % was obtained, but this value was higher than when fructose was used on its own. So, although there was a dilution effect, other fructose pathways are likely to have occurred.

The result with only glucose shows that only 2.5 mol % of HMF is formed (Table 1 entry 6) because of the lack of Lewis acid sites in the HSO_3Cl catalyst.[40] However, the HMF yield

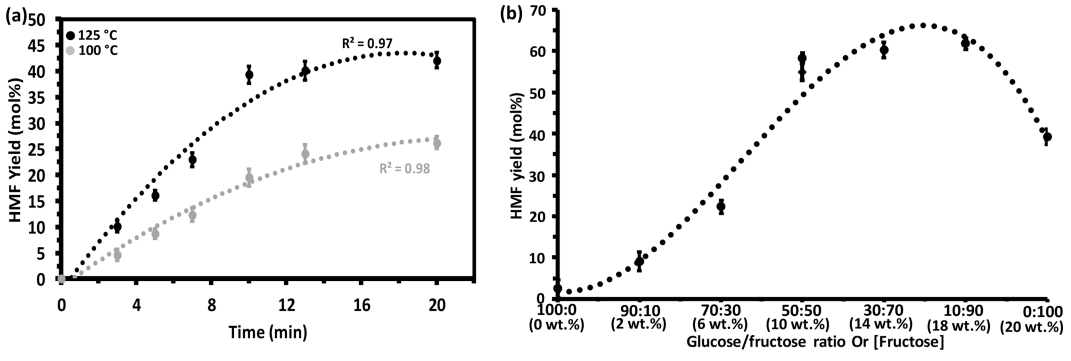

Figure 3. (a) Effect of reaction time for the conversion of concentrated fructose to HMF in monophasic systems (1.01 g of fructose, 1.00 g of [BMIM]Cl, and 0.05 g of catalyst) and (b) relationship between glucose/fructose ratio with HMF yield (1.01 g of substrate, 1.00 g of [BMIM]Cl, 0.05 g of catalyst, and 3.00 g of MeTHF; 125 °C; 10 min).

https://doi.org/10.1021/acsomega.3c05060
ACS Omega 2023, 8, 40442−40455

Table 1. Conversion of Sugars (20 wt %) to HMF in Different Reaction Conditions[a]

	substrate/solvent system	temp. (°C)	time (min)	HMF yield[b] (mol %)	HMF selectivity[c] (mol %)	C6 dimers[d] (mol %)	DFA (or similar isomeric compound)[d] (mol %)	glucose (mol %)	fructose (mol %)	fructose conversion (mol %)	Glucose conversion (mol %)	Others[e] (mol %)
1.	fructose/monophasic	100	10	19.5	31.3		28.1			94.2	---	---
2.	fructose/monophasic	125	10	36.3	37.0		24.3			98.1	---	---
3.	fructose/biphasic	100	10	37.7	37.9		25.7			99.4	---	---
4.	fructose/biphasic	125	10	39.3	39.4		21.4			99.9	---	---
5.	fructose/biphasic[f]	125	10	46.2	46.3		17.3			99.7	---	---
6.	glucose/biphasic	125	10	2.5	2.6	5.5		35.0			58.9	0.2
7.	glucose/biphasic[f]	125	10	7.8	12.4	7.2		31.3			62.8	0.3
8.	sucrose/biphasic	125	10	55.0	55.9	12.4	3.7	23.4	0.3		---	0.3
9.	glucose + fructose (90:10)/biphasic	125	10	9.1	9.1/22.9[e]	9.3		42.7	0.1	99.5	39.8	0.3
10.	glucose + fructose (70:30)/biphasic	125	10	22.3	22.5/48.8	8.4		30.2	0.1	99.2	45.7	0.3
11.	glucose + fructose (50:50)/biphasic	125	10	58.4	58.5/73.9	6.9	9.0	24.3	0.2	99.8	79.1	0.3
12.	glucose + fructose (30:70)/biphasic	125	10	60.3	62.1/72.5		10.7	12.4	1.2	97.1	83.2	0.3
13.	glucose + fructose (10:90)/biphasic	125	10	61.8	62.2/69.5		11.3	2.3		99.3	88.9	0.2
14.	sucrose[g]/biphasic	125	10	10.7	19.3		15.4	20.3	0.6		---	---
15.	sucrose[h]/biphasic	125	10	15.4	25.5		17.2	21.2	0.6		---	---
16.	sucrose[i]/biphasic	125	10	30.8	43.4		6.1	28.8	0.4		---	0.4
17.	sucrose[j]/ biphasic	125	10	66.8	68.7	6.5		15.3			---	1.2
18.	sucrose/biphasic	125	3	2.1	4.3		8.4	26.7	0.4		---	---
19.	sucrose/biphasic	125	5	12.8	21.6		7.8	25.2	0.4		---	---
20.	sucrose/biphasic	125	7	32.0	40.8		6.4	24.3	0.3		---	---

[a]In the monophasic system, 0.262 g fructose, 1.00 g [BMIM]Cl, and 0.05 g catalyst were used. In the biphasic system, 1.01 g substrate, 1.00 g [BMIM]Cl, 0.05 g catalyst, and 3.00 g MeTHF were used. [b]HMF yield in [BMIM]Cl/MeTHF phases. [c]HMF selectivity according to fructose/glucose. [d]Quantification of dimers based on HPLC (dimer peaks were identified based on unique LCMS peaks; see Section 2.3). [e]Organic acid byproducts (formic acid, acetic acid, and levulinic acid). [f]Sugar concentrations at 18 wt % (substrate, 0.91 g; [BMIM]Cl, 1.00 g; catalyst 0.05 g; and MeTHF, 3.00 g). [g]Sucrose conversion without any catalyst. [h]Sucrose conversion by using unsulfonated carbon. [i]Sucrose conversion in water/MeTHF. [j]Sucrose conversion using 0.05 M HCl.

https://doi.org/10.1021/acsomega.3c05060
ACS Omega 2023, 8, 40442−40455

Table 2. Comparison of Various Catalysts in the Conversion of Concentrated Sugars to HMF

entry	substrate	sugar concentration (%)	catalyst	solvent/s	reaction conditions			ref
					temp. (°C)	time (min)	HMF yield (%)	
1.	glucose	8.83 [80][a]	CrCl3	ionic liquid/organics/ water	108	60	64.5	7
2.	glucose	[10]	$CrCl_2$	[EMIM]Cl	100	180	70.0	62
3.	glucose	9.15 [80]	$SnCl_4$	[b]GDE/[EMIM]Br	100	120	58.7	44
4.	fructose	9.15 [80]	$SnCl_4$	GDE/[EMIM]Br	100	120	63.5	44
5.	sucrose	9.15 [80]	$SnCl_4$	GDE/[EMIM]Br	100	180	65.7	44
6.	glucose	[30]	$1.5Sn/Al_2O_3$	[EMIM]Br	140	60	50.8	19
7.	fructose	[30]	$1.5Sn/Al_2O_3$	[EMIM]Br	140	60	69.1	19
8.	sucrose	[30]	$1.5Sn/Al_2O_3$	[EMIM]Br	140	180	63.0	19
9.	glucose	[30]	$1.5Sn/Al_2O_3$	[EMIM]Br	140	180	55.7	19
10.	glucose	[10]	$SnPO_4$	[EMIM]Br	120	180	58.3	8
11.	glucose	[10]	Al_2O_3	[EMIM]Br	120	180	49.7	63
15.	fructose	[10]	HT carbonaceous glucose	[BMIM]Cl	100	60	75.1	49
16.	fructose	[9]	CSS	[BMIM]Cl	80	20	76.0	50
17.	fructose	[10]	lignin-SO_3H	[BMIM]Cl	100	10	93.4	54
18.	fructose	4.76 [10]	lignin-SO_3H	[BMIM]Cl/DMSO	110	10	84	53
19.	glucose	4.76 [10]	lignin-SO_3H	[BMIM]Cl/DMSO	160	50	68	
20.	sucrose	[10]	cellulose-C	[BMIM]Cl	160	15	62.7	51
21.	fructose	[20]	yeast-C	[BMIM]Cl	80	30	83.5	52
22.	sucrose	[10]	yeast-C	[BMIM]Cl	80	30	44.8	
23.	fructose	[20]	CM-SO_3H	[BMIM]Cl	80	30	83.5	
28.	fructose	20 [100]	sulfonated carbon	[BMIM]Cl/[c]MeTHF	125	10	39.3	this work
29.	glucose	20[100]	sulfonated carbon	[BMIM]Cl/MeTHF	125	10	2.5	this work
30.	sucrose	20 [100]	sulfonated carbon	[BMIM]Cl/MeTHF	125	10	55.0	this work
31.	sucrose	20 [100]	*p*-TsOH carbon	[BMIM]Cl/MeTHF	125	10	23.8	this work
32.	glucose/fructose	20 [100]	sulfonated carbon	[BMIM]Cl/MeTHF	125	10	58.4	this work

[a]Relative to [EMIM]Cl, 1-ethyl-3-methylimidazolium chloride ionic liquid medium. [b]GDE, glycol dimethyl ether. [c]MeTHF, 2-methyltetrahydrofuran.

increased to 7.8 mol % in 18 wt % glucose concentration because of the dilution effect. Therefore, the dehydration reaction is enhanced in concentrated sugar solutions where glucose is present with fructose either covalently bonded (i.e., sucrose) or as a mixture. When glucose is present in the mixture, small amounts of byproducts formic acid, levulinic acid, and acetic acid are obtained.[41,42] The formation of formic acid and levulinic acid may be due to the rehydration of HMF.[43] Formic acid and levulinic acid are weak acids that can act as Brϕnsted acids in the conversion of fructose to HMF. However, the Brϕnsted acidic effect of formic acid and levulinic acid in the dehydration of fructose to HMF is not significant because they are present in low concentrations (<0.4%). Besides, with glucose on its own, formic acid and acetic acids are also formed, yet the HMF yield is low. Only 10.7 mol % of HMF is produced in the absence of any catalyst (Table 1 entry 14), and a slightly higher value (15.6 mol %) is produced with unsulfonated carbon catalyst (Table 1 entry 15). When water was used as a solvent (Table 1 entry 16) in place of [BMIM]Cl, the HMF yield was lower, indicating that [BMIM]Cl plays a role in sucrose conversion to HMF, in part because of its acidic nature.[44] However, in the aqueous medium, higher concentrations of formic acid and levulinic acids are formed compared to [BMIM]Cl due to the rehydration of HMF in the aqueous media.[45] So, there are likely other reactions that are responsible for the increased HMF yield with the addition of glucose to concentrated fructose solution in the biphasic system. Because of the adverse effects of water, high-fructose corn syrup (HFS) was not tested in this catalytic system even though it is cheaper and readily available in different fructose concentrations (HFS 55 and HFS 95). In the present study, the increase in HMF yield with glucose/fructose of 50:50 to up to 10:90 is small; thus, it would be economically beneficial to use a 50:50 glucose to fructose ratio in an industrial setting due to the higher cost of fructose.

The catalyst efficiency of sulfonated carbon was compared with various catalytic systems used for the conversion of concentrated sugars to HMF in IL media (Table 2). As previously mentioned, Lewis acid based catalysts such as Cr, Sn, and Al salts and oxides are used mainly because of their ability to isomerize glucose to fructose.[7,44] Further, Cl^- ions in the IL form H-bonds with −OH groups of the sugars, and the Lewis acid metal sites interact with O atoms in the −OH groups and promote the formation of acyclic glucose.[46] The catalyst $CrCl_3$ has resulted in 65% HMF yield from highly concentrated glucose in an IL−organics−water media. Moreover, over Sn^{4+} catalysts, apart from glucose isomerization, dehydration of fructose to HMF occurs because of the Brϕnsted acid nature of the Sn−OH groups.[47] However, despite the effectiveness of this type of catalysts, apart from the toxicity issues, their reusability is a significant disadvantage.[48] Therefore, carbonaceous catalysts have gained much attention due to their cheap carbon precursors, easy synthesis, and improved chemical stability. Qi et al.[49] derived a carbon catalyst by hydrothermal carbonization of glucose and observed 75.1% HMF yield from fructose dehydration (10 wt % concentration) at 100 °C after 60 min. Cellulose-derived

https://doi.org/10.1021/acsomega.3c05060
ACS Omega 2023, 8, 40442−40455

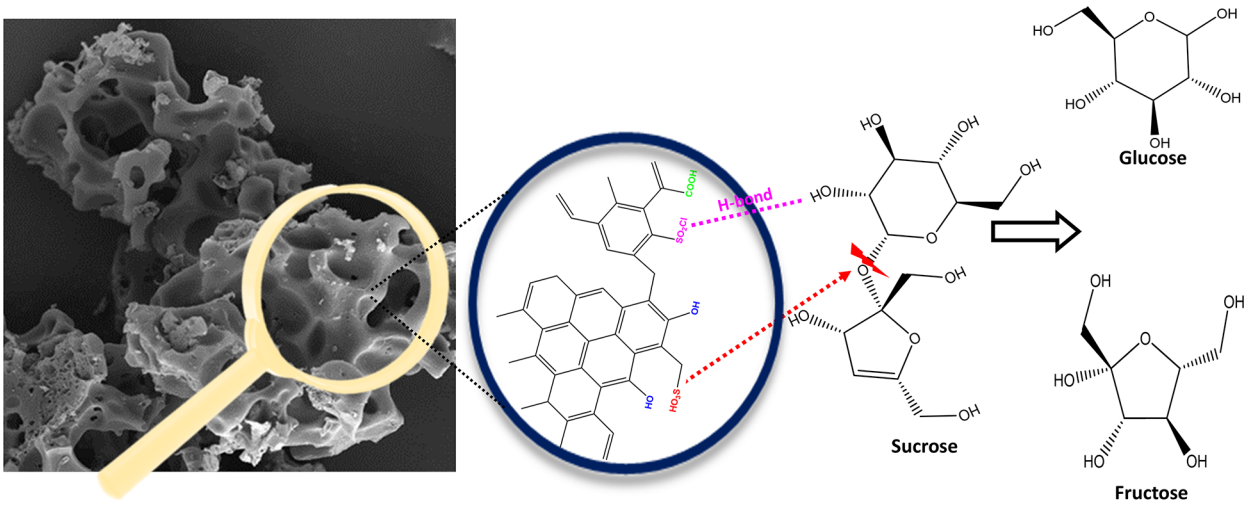

Figure 4. Proposed molecular structure of the HSO_3Cl catalyst and hydrolysis of sucrose to its monomers.

Table 3. Total Acid Strength and Distribution of Acid Sites of the Carbon Catalysts

catalyst	total acidity (mmol)	−COOH		−OH		$-SO_3H/-SO_3^-$		pore properties	
		XPS at. %	titration (mmol g^{-1})	XPS at. %	titration (mmol g^{-1})	XPS at. %	titration (mmol g^{-1})	SSA (m^2g^{-1})	V_{total} ($cm^3 g^{-1}$)
HSO3CI catalyst	5.01	5.58	1.34	9.39	0.90	1.89/1.37	2.77	527	0.28
after the 4th recycle	4.22	9.10	1.39	14.74	1.02	0.52/1.47	1.81	468	0.13
regenerated catalyst	4.89	4.97	1.28	8.43	0.85	1.74/1.56	1.62	507	0.18
p-TsOH	3.41	12.96	1.02	34.36	1.08	0.94/0.69	1.31	241	0.14

carbon catalysts were synthesized by Qi et al.[50] and Hu et al.[51] and employed in fructose and sucrose conversion (9 wt % concentration) to HMF, and they observed 76 and 62.7% HMF yields, respectively. Moreover, yeast-derived carbon catalysts were also studied in the conversion of fructose (20 wt % concentration) and sucrose (10 wt % concentration) to HMF, and yields of 83.5 and 44.8%, respectively, were observed.[52] Further, Xie et al.[53] studied the conversion of sugars (10 wt % concentration) to HMF using sulfonated carbon catalyst in [BMIM]Cl media and observed a 93.4% HMF yield. Guo et al.[54] also investigated the catalytic effect of lignin-derived sulfonated carbon in a [BMIM]Cl/DMSO biphasic system and observed 84 and 68% HMF yields from fructose and glucose (4.76 wt % concentration). However, our sulfonated carbon catalyst, devoid of any metal inclusion, gave a relatively high HMF yield (61.8%) with greater sugar loadings (20 wt % concentration).

Shen et al.[55] and Shuai and Pan[56] have studied cellulase mimitic heterogeneous catalysts containing −Cl and $-SO_3H$ groups in the conversion of cellulose to HMF and to levulinic acid. They observed that −Cl groups acted as cellulose-binding sites and $-SO_3H$ groups acted as catalytic sites. However, the HSO_3Cl catalyst derived from CGT also contains $-SO_2Cl$ and $-SO_3H$ groups that can mimic the sucrase enzyme in the conversion of sucrose to HMF in which sucrose molecules are adsorbed to the HSO_3Cl catalyst via hydrogen bonds among hydroxyl groups of sucrose and electronegative −Cl groups of the HSO_3Cl catalyst and sucrose is further hydrolyzed to HMF by $-SO_3H$ groups (Figure 4).[55] The suggested molecular structure for the sulfonated carbon catalyst is a modification of the structure previously proposed for this catalyst[12] (Figure 4). Moreover, Yan et al.[57] claimed that phenolic −OH groups favor the isomerization of glucose to fructose. Our sulfonated catalyst has a low −OH group content, so it would contribute to low isomerization potential. Kitano et al.[58] and Suganuma et al.[59] suggested that SO_3H and −COOH groups function as Brønsted acid sites and hydrolyze sucrose to its monomers and dehydrate fructose to HMF (Figure S5). The effect of sulfonation was examined (Table 1 entry 15), and the low HMF yields confirmed the functionality reported in the literature.

The effect of sulfonation of the carbon with chlorosulfonic acid was compared with *p*-TsOH sulfonation, and only 23.8 mol % of HMF was produced with the *p*-TsOH-derived catalyst (Table 2 entry 31). The reason for the low activity is in part due to lower total acidity (3.41 vs 5.01 mmol g^{-1}) and also lower $-SO_3H/-SO_3^-$ acid sites (1.31 mmol g^{-1}, Table 3) despite having ∼90% more S content than the chlorosulfonic-acid-derived carbon catalyst (Table S2). The high-resolution-S XPS of the *p*-TsOH catalyst (Figure S6) shows the presence of two additional peaks relating to S−S/C═S and −C−S, which are not active and effective in the conversion of sucrose to HMF.[60] Moreover, the homogeneous catalytic effect was compared to the HSO_3Cl catalyst using HCl (0.05 M) for the conversion of sucrose to HMF, and an HMF yield of 66.8 mol % was observed (Table 1 entry 17). In this reaction, sucrose hydrolyzed easily to its monomers and dimerized only into glucose−glucose (6.5 mol %) due to their high concentration. Moreover, Binder and Raines[61] have observed the adverse effect of chloride anions in preventing or disturbing the formation of fructose oligomers in dimethylacetamide (DMA)/LiCl reaction media.

https://doi.org/10.1021/acsomega.3c05060
ACS Omega 2023, 8, 40442−40455

2.3. Proposed Reaction Mechanism. The reaction products formed with the concentrated sugar solutions were investigated by HPLC (Figure 5) and LCMS (Figures S7−S11 and Table S3). The HPLC chromatograms show new peaks for reactions with both fructose (9.5 min) and glucose (9.0 min). These peaks were also obtained with sucrose (Figure 5). As the 9.0 min retention time of one of these intermediates is similar to sucrose, it was inferred that these molecules are the reversion products or dimers of glucose and fructose, which have the isomeric structure of sucrose.[64] The peak at 9.5 min is inferred to be DFA (or a similar isomeric structure) based on the prevalence of fructose and subsequent LCMS analysis. Although dimer peaks can be due to artifacts in the analytical technique when analyzing concentrated solutions, this was ruled as unlikely as the MS results showed that the dimer concentrations differed with changing reaction conditions. Additionally, the product mixture was diluted (10-fold) and reanalyzed by HPLC, and similar peaks corresponding to dimer structures with reduced intensities were observed.

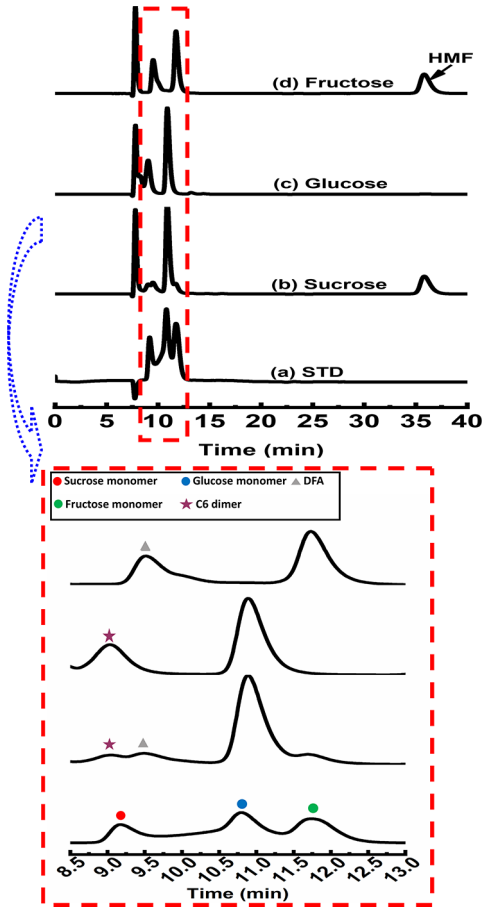

Figure 5. HPLC chromatograms of concentrated (20 wt %) sugar dehydration to HMF at 125 °C in 10 min (sugars, 1,01 g; [BMIM]Cl, 1.00 g; catalyst, 0.05 g).

The LCMS spectra of concentrated fructose, glucose, and sucrose standard solutions are shown in Figure S7, and the differences in retention times between HPLC and LCMS were due to the different chromatographic conditions (different columns, column temperatures, and different solvents). As observed in Figure S7, fructose and glucose standard solutions mainly show a peak corresponding to their monomeric structures at m/z 203. Further, concentrated sucrose depicted a significant peak in the ion chromatogram (Figure S7) for an m/z value of 365.1. However, when the concentrated fructose, glucose, and sucrose solutions were analyzed by LCMS after reaction, peaks that have an nm/z value of 365.1 (Figures S8 and S9) were observed. The intermediates observed in LCMS may correspond to the Na^+ adduct of sucrose or the Na^+ adduct of the DFA, dimers, or reversion products of glucose or fructose. The metallic Na^+ ions are present in water and in the instrument's metallic surfaces, which are enough to ionize the compounds entering the mass spectrometer in small amounts (nanomoles). Therefore, both monosaccharides might have dimerized and produced isomerized forms that have the same molecular weight as sucrose. Tan-Soetedjo et al.[65] suggested the formation of neotrehalose (which has the same molecular weight as sucrose), a reversion dimer of glucose produced at high sugar loadings. In the mechanism of reversion product formation, a carbocation is formed at the C1 position of glucose that could react with the −OH group of another sugar molecule to form a disachcharide.[66] However, on the basis of the stereochemistry and different bonding of carbocations and −OH groups in β- and α-glucose molecules, there are 11 different possible dimer structures (neotrehalose, isotrehalose, etc.).[66]

Furthermore, Thompson et al.[67] listed several isomeric structures of sucrose that are formed because of glucose−glucose or glucose−fructose dimerization. Many others[68−70] also identified DFA as an intermediate product in the dehydration of fructose to HMF, which is formed by the removal of a water molecule from the dimer. The ion at m/z 347.10 (Figure S12d) corresponds to the Na^+ adduct of DFA or similar isomeric compound that is produced from the dehydration of the C6 dimers (Figures S8, S10, and S11c,d). This peak at m/z 347 is present only in the solutions of sucrose and fructose, suggesting that the dehydration product involves fructose. Further, the involvement of fructose in the dehydration products was confirmed by reacting an equimolar ratio of glucose and fructose and with peaks observed corresponding to ions at m/z values of 365.11 and 347.10.

Another peak is observed at m/z 527, mainly for glucose reactions, and it corresponds to the trimer structure. Therefore, it could be inferred that, in the conversion of concentrated glucose to HMF by the sulfonated carbon, the glucose molecule has undergone dimerization and trimerization. Moreover, Pilath et al.[66] have also observed the formation of glucose dimers and oligomers at a high glucose concentration (20 wt %) in H_2SO_4 acid (1.2 wt %) media. The peak observed at m/z 219 is unusual, but sometimes, fragmentations are driven by the stability of the neutral product, as shown in Figure S12h. So, it is plausible that such dimers are formed under the experimental conditions and may be more susceptible to transformation to HMF where the fructose molecule is present either covalently bonded to glucose or in a mixture. Therefore, possible structures for the observed major m/z values in the LCMS spectra of concentrated sugar solutions are suggested in Figure S12.

Shorter reaction times (3, 5, and 7 min) were conducted with a concentrated sucrose solution to establish kinetic information on the dimers (Table 1 entries 18−20). A peak was observed around 9.5 min in the HPLC spectra (Figure 5) representing the formation of the isomerized form of DFA. So, although glucose−fructose and glucose−glucose dimers form at times from 10 min, only DFA isomers are formed at shorter

https://doi.org/10.1021/acsomega.3c05060
ACS Omega 2023, 8, 40442−40455

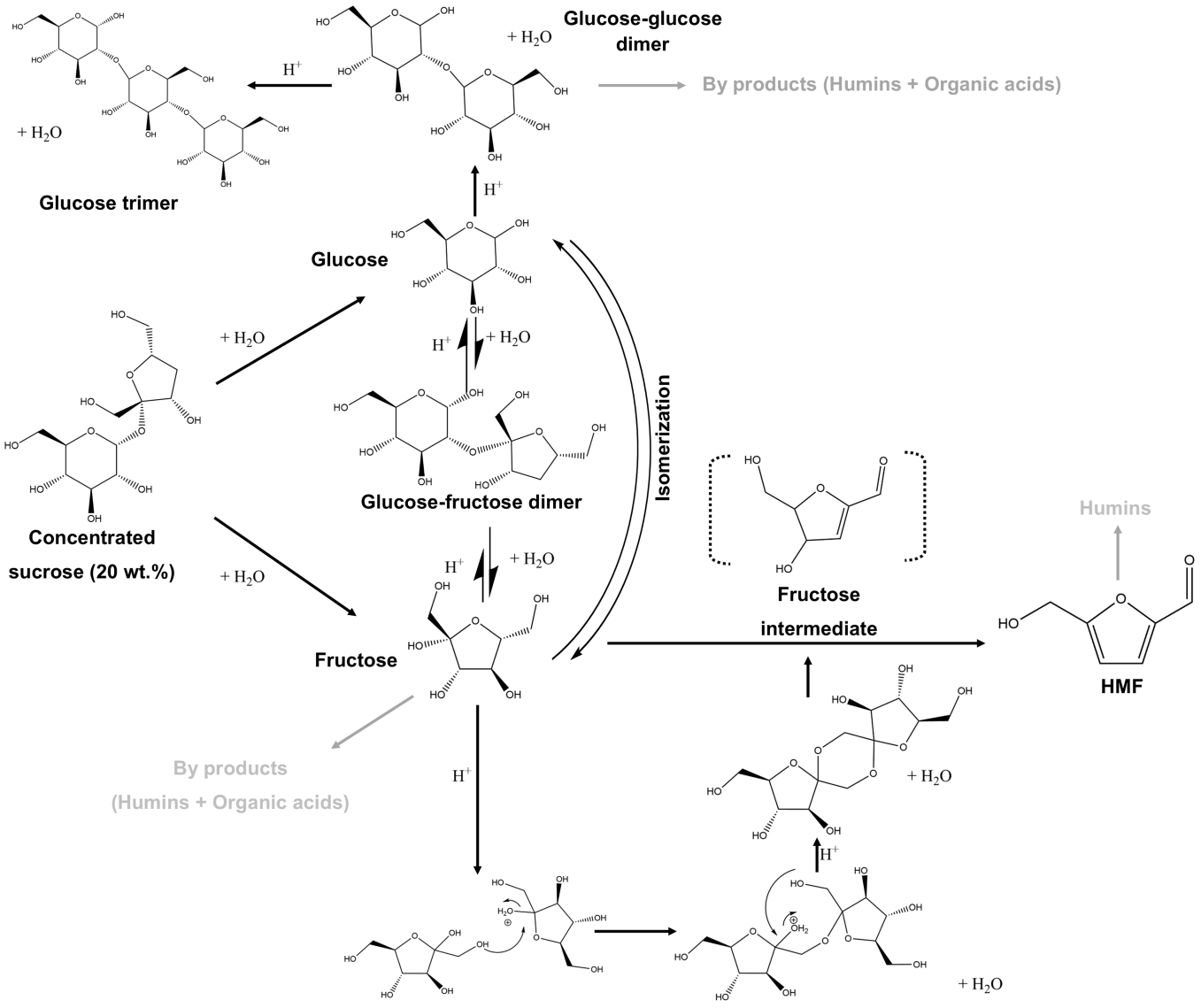

Figure 6. Suggested reaction pathways for the conversion of concentrated sucrose to HMF with the carbon catalyst in the [BMIM]Cl/MeTHF biphasic system.

reaction times, revealing the higher reactivity of fructose monomers than glucose monomers.[39] This offers the explanation that when glucose is present in a solution of glucose−fructose mixture or as covalently bonded monomer in sucrose, the reactive fructose couples with glucose to form the more stable glucose−fructose dimer, a sucrose isomer, which subsequently undergoes further reactions in its transformation to HMF. Proposed reaction pathways for the conversion of concentrated sucrose to HMF are shown in Figure 6.

As reported, fructose on its own (20 wt %) resulted in an HMF yield of 39.3 mol %, but the yield increased to 46.2 mol % when the fructose concentration was reduced to 18 wt %. In general, concentrated sugar solutions result in lower HMF yields due to mass transfer limitations and the prevalence of byproduct reactions. Therefore, the dilution effect of glucose in the glucose/fructose of 10:90 only played a minor role in the high yield of HMF (61.8 mol %) obtained in the system. So, it may be inferred that glucose−fructose dimers contributed to the increase in HMF yield perhaps by inhibiting the formation of byproducts (Figure 7). This may have been achieved by reducing the concentration of other intermediates that lead to byproduct formation, with this phenomenon more prevalent in concentrated sugar solutions.

Another peak was observed in the HPLC spectra of all of the sugar solutions at around 48 min. This peak decreased in intensity with increasing time, perhaps suggesting that it functions as an intermediate that leads directly to the formation of HMF. The LCMS analysis of concentrated sucrose solution shows a peak with 145.05 mass that corresponds to the H^+ adduct of the fructose intermediate 4-hydroxy-5-hydroxymethyl-4,5-dihydrofuran-2-carbaldehyde (Figure S13).[71] To confirm the fructose intermediate, a dilute fructose solution (4.54 wt %) was converted to HMF by varying the reaction time up to 20 min, and it was observed that this peak decreased with the reaction time (Figure S14).

2.4. Reusability of the Catalyst. Compared with homogeneous catalysts, one of the significant properties of heterogeneous solid catalysts is their reusability. The stability of the HSO_3Cl catalyst was experimented in the conversion of concentrated sucrose to HMF at 125 °C for 10 min. As observed in Figure 8, the HMF yield gradually decreased from 56 to 43 mol % in the fifth recycle test. The total acid strength

https://doi.org/10.1021/acsomega.3c05060
ACS Omega 2023, 8, 40442−40455

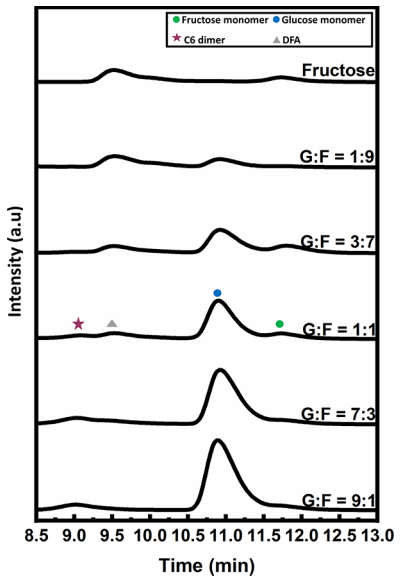

Figure 7. Effect of the glucose/fructose ratio on glucose and fructose and dimer formation (1.01 g of substrate, 1.00 g of [BMIM]Cl, 0.05 g of catalyst, and 3.00 g of MeTHF).

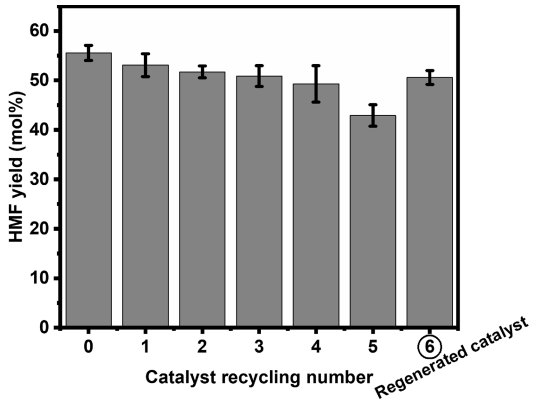

Figure 8. Catalyst reusability tests in the conversion of concentrated sucrose to HMF at 125 °C for 10 min (1.01 g of substrate, 1.00 g of [BMIM]Cl, 0.05 g of catalyst, and 3.00 g of MeTHF).

of fresh and recycled catalysts (after four recycles) was measured by Bohem titration, and a 0.79 mmol g^{-1} reduction was observed that could be due to the catalyst deactivation. Two main possibilities for the catalyst deactivation are (i) the leaching of $-SO_3H$ functional groups or (ii) the adsorption of humins onto the active sites.[55] The concentration of $-SO_3H$ sites (the primary active sites) was measured in fresh and recycled HSO_3Cl catalyst after the fourth recycle by titration and XPS analysis, and a 20−30% loss was observed (Table 3). Further, the S content of the catalyst after the fourth recycle was compared with the fresh catalyst, and only 0.20% S reduction was observed (Table S2). The affinity of the $-SO_3H$ groups for the carbon catalyst was analyzed by the hot filtration method. Reaction using the filtrate (leachate from filtering the catalyst) in the biphasic system observed only 5.21 mol % HMF yield compared to 3.12 mol % HMF yield without any catalyst. Therefore, $-SO_3H$ groups that leached from the HSO_3Cl catalyst resulted in only a small increase in the HMF yield. Therefore, it could be inferred that $-SO_3H$ groups have strong bonding and high affinity with the carbon catalyst, and deactivation of the catalyst has not occurred to a significant extent due to leaching. When considering the total carbon content of the catalyst after the fourth recycle, a 13% increase was observed compared to that of the fresh HSO_3Cl catalyst (Table S2). Therefore, the morphology of the recycled HSO_3Cl catalyst was observed by the SEM image, which showed (Figure 9b) coagulated particles of a similar nature to

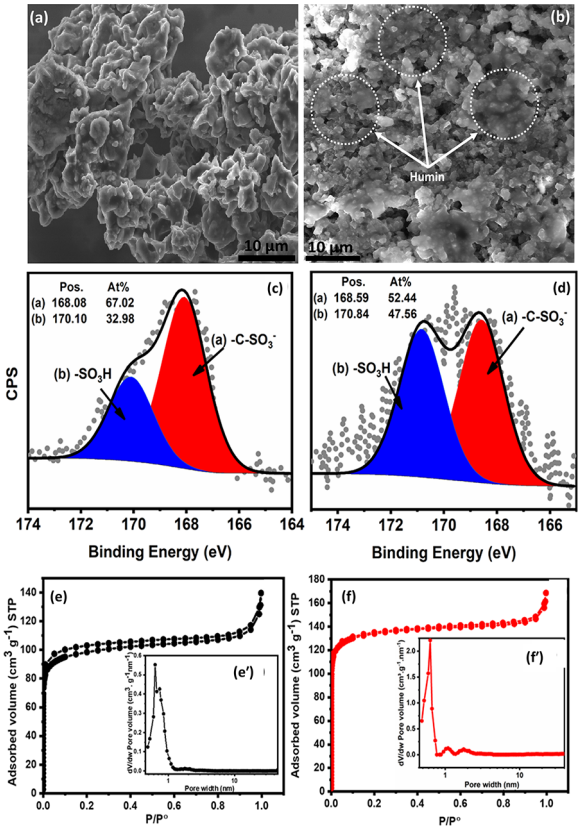

Figure 9. (a) SEM image of the fresh HSO_3Cl catalyst, (b) SEM image of the HSO_3Cl catalyst after the fourth recycle, (c) XPS wide spectrum of the spent catalyst, (d) XPS wide spectrum of the spent catalyst after regeneration, (e) N_2 adsorption−desorption isotherms and pore size distribution of the spent catalyst, and (f) N_2 adsorption−desorption isotherms and pore size distribution of the regenerated catalyst.

humins reported in the literature.[72] Further, the fresh catalyst's BET surface area and total pore volume were reduced to 468 and 0.38 cm^3 g^{-1} after four recycle runs because of the blocked pores by humins (Table 3). The presence of carbon in the reaction medium was analyzed by measuring the total organic content (TOC) and was found to increase by >200 mg L^{-1} after the fourth recycle (Figure S15). Huo et al.[72] reported the effective regeneration of carbon supported catalysts by oxidation in air. Thus, the HSO_3Cl catalyst, after its fifth recycle run, was regenerated by oxidizing in air at 200 °C for 30 min. After regeneration, total acidity and the amount of $-SO_3H$ groups increased to 4.89 mmol g^{-1} and 1.74 at. %, respectively (Table 3 and Figure 9d). Moreover, regeneration increased the total surface area of the spent catalyst up to 507 cm^3 g^{-1} (Figure 9f). The regenerated catalyst resulted in a comparable HMF yield to the fresh catalyst by effectively adsorbing sucrose molecules into its surface and reacting with $-SO_3H$ and other functional groups to produce HMF. Regeneration of the HSO_3Cl catalyst at a mild temperature

https://doi.org/10.1021/acsomega.3c05060
ACS Omega 2023, 8, 40442−40455

for a shorter time is a simple but effective process that can be performed to improve its activity.

3. CONCLUSIONS

Biomass-derived carbon catalysts have gained much interest due to their low cost and good performance. This study investigated utilization of a sulfonated catalyst derived from CGT that provided satisfactory yields of HMF with 20 wt % sugar solutions. Interestingly, the yield of HMF was higher in the concentrated sucrose solution and glucose/fructose mixtures than in the concentrated fructose solution on its own. The formation of glucose−fructose dimers in these systems enhanced the HMF formation. So, a strategy of adding glucose to concentrated fructose solutions may be a simple way to increase the HMF yield at high sugar concentrations. As observed in this study, a 10:90 weight ratio of glucose/fructose resulted in the highest HMF yield, although the equimolar ratio also gave a similar HMF yield. Therefore, on an industrial scale, an equimolar ratio of glucose and fructose could be used to reduce operating costs. The sulfonated catalyst showed good reusability. In a future study, it will be worth investigating carbon catalysts derived from biomasses containing endogenous or inorganic metal ions such as Al and Fe to increase Lewis acid sites to support the isomerization reaction. Carbon catalysts with different pore sizes and surface areas with this functionality should be studied to identify and further optimize the catalyst properties that can provide faster kinetics and effective mass transfer for very high sugar concentrations. Also, studies with cellulosic glucose at higher sugar concentrations after partial isomerization to fructose and conversion of the mixture to HMF should be explored.

4. EXPERIMENTAL DETAILS

4.1. Materials and Chemicals. Milled (2.0 mm particle size) and air-dried (24 h at 45 °C) CGT was analyzed for its total carbohydrate content of cellulose and hemicellulose and its lignin content by the acid hydrolysis method as described in the National Renewable Energy Laboratory procedures.[73] D-(+)-Fructose, D-glucose, sucrose, 1-butyl-3-methylimidazolium chloride ([BMIM]Cl), *p*-toluenesulfonic acid (*p*-TsOH), and 2-methyltetrahydrofuran (MeTHF) were obtained from Sigma-Aldrich (Castle Hill, NSW, Australia). Methanol, KOH, HSO_3Cl, HCl (32 wt %), phenolphthalein, and reagent-grade DMSO were purchased from Merck (Kilsyth, Victoria, Australia). The [BMIM]Cl was oven-dried for 1 h at 105 °C prior to use.

4.2. Synthesis of the Sulfonated Catalyst. The sulfonated catalyst was prepared as discussed in our previous work,[12] in which 2 M HCl treated ball-milled CGT was activated with KOH (1:2 weight ratio) by carbonizing at 400 °C by 3 °C min^{-1} and holding for 1 h at 400 °C in a tube furnace under a N_2 atmosphere. Then, the carbonized sample was sulfonated after HCl washing and drying at 105 °C for 24 h. In the sulfonation process, 5 mL of dichloromethane and 150 μL of chlorosulfonic (HSO_3Cl) acid were added to 100 mg of the carbonized sample and stirred for 9 h at room temperature. The sample was washed with methanol and deionized water four times and dried for 8 h at 70 °C.[74] For comparison, the sulfonated catalyst derived from para-toluene sulfonic acid (*p*-TsOH) was prepared by the acid digestion method in a 25 mL Parr reactor by mixing 2 g of the CGT carbon material with 8 g of *p*-TsOH acid at 180 °C for 24 h.[74,75]

4.3. Catalyst Characterization. Nitrogen adsorption−desorption analysis was performed at 77 K using a Micrometrix 3-flex 2020, and the sample was degassed overnight at 200 °C prior to the analysis. The total surface area, total pore volume, and micropore surface area of the catalyst were calculated according to the Brunauer−Emmett−Teller (BET) method. The powder X-ray diffraction (XRD) patterns were collected using a Bruker D8 Advance powder diffractometer (Co $K\alpha_1$ radiation, λ = 1.7890) under 35 kV and 40 mA operating conditions. The curve fittings and deconvolution of the XRD pattern were performed by using the Origin Pro 9.1.0 software.[76] The Raman analysis was conducted by using a Renishaw Raman microscope under a 532 nm laser wavelength. X-ray photoelectron spectra (XPS) were acquired using a KRATOS AXIS Supra spectrometer with Al Kα radiation, and the C 1s peak at 285 eV was used as the reference peak to calibrate XPS spectra. The total acidity and $-SO_3H$ (and SO_3^-), −OH, and −COOH acid site concentrations were analyzed by the titration method discussed by Boehm.[77] The total acidity was measured by titrating the ultrasonicated mixture of 0.05 g of catalyst and 20 mL of NaOH (0.01 mol dm^{-3}) with 0.01 mol dm^{-3} HCl solution. The concentration of the $-SO_3H$ groups was measured by centrifuging the ultrasonicated mixture of 0.05 g of catalyst and 20 mL of NaCl solution (0.01 mol dm^{-3}) and titrating the supernatant with NaOH solution (0.01 mol dm^{-3}). The concentrations of $-SO_3H$ and −COOH groups were measured by titrating the supernatant of the centrifuged mixture of 0.05 g of catalyst and 20 mL of Na_2CO_3 (0.01 mol dm^{-3}) after ultrasonication of the catalyst in HCl solution (0.01 mol dm^{-3}). The titrations were performed by using phenolphthalein as the indicator. The solid-state NMR (SSNMR) of the catalyst was performed using a Bruker Advance III Spectrometer with a double air bearing MAS probe and 300 MHz magnets. The cross-polarization magic angle spinning (CPMAS) spectra were measured at 100 kHz frequency with 1.5 ms optimum time and 3 s relaxation time. The morphology of the carbon catalysts was analyzed using scanning electron microscopy (SEM) images obtained by JEOL 7001F FESEM, and the elemental distributions were analyzed by energy-dispersive X-ray spectroscopy (EDS) data obtained from the Oxford X-Max 80 mm^2 SDD detector. The drift-FTIR spectra of the sulfonated and unsulfonated carbons were collected on a Thermo-Nicolet iS50 ABX FTIR spectrometer equipped with a DLaTGS detector (gain: 8) using a Specac MiniDiff DRIFT accessory. The samples were prepared as a 100-fold dilution in spectroscopy-grade KBr and ground using an agate mortar and pestle that was sparsely cleaned with KBr. A total of 256 scans were collected at 4 cm^{-1}, the resultant spectra were converted into Kubelka−Munk before autobaseline, and atmospheric suppression algorithms were applied.

4.4. Conversion of Concentrated Sugars to HMF. Reagents were added into a thick-walled glass pressure tube and sealed with a polytetrafluoroethylene plug. For 20 wt % concentrated sugar solution, the monophasic systems consisted of sugars (0.262 g), carbon catalyst (0.05 g), and [BMIM]Cl (1.00 g), whereas the biphasic systems consisted of sugars (1.01 g), carbon catalyst (0.05 g), [BMIM]Cl (1.00 g), and 3.5 mL (3.00 g) of MeTHF. The reaction mixture was continuously stirred at 800 rpm in a heated oil bath for the desired temperature and time. The reactor was cooled in a

https://doi.org/10.1021/acsomega.3c05060
ACS Omega 2023, 8, 40442−40455

water bath to ambient temperature at the end of the reaction, and the mixture was diluted with MeTHF (15 mL) and water (100 mL) prior to phase separation. The MeTHF and IL phases were filtered with 0.45 μm polytetrafluoroethylene filters prior to analysis by high-performance liquid chromatography (HPLC) to determine the concentrations of sugars, HMF, and byproducts. The sugar conversion, HMF yield, and selectivity were calculated according to the following equations:[78,79]

$$\text{Conversion}\left(\text{mol\%}\right) = \left(\frac{\text{moles of sugar reacted}}{\text{moles of starting sugar}}\right) \times 100\% \quad (2)$$

$$\text{Yield(mol\%)} = \left(\frac{\text{moles of the product}}{\text{moles of starting sugar}}\right) \times 100\% \quad (3)$$

$$\text{Selectivity(mol\%)} = \left(\frac{\text{yield}}{\text{conversion}}\right) \times 100\% \quad (4)$$

4.5. Identification of Sugars, Dimers, and Sucrose Isomer. The formation of the sugar, dimers, and sucrose isomer was monitored by both HPLC and liquid chromatography−mass spectroscopy (LCMS). The HPLC system (Waters e2695 Model) utilized an 87H Aminex analytical column and was equipped with UV 210/280 nm detectors and refractive index (RI) detector (Waters 410). A 20 μL sample injection was used. The column temperature was set at 60 °C, and the mobile phase was 0.5 mM H_2SO_4 set at a flow rate of 0.5 mL min^{-1}. In the LCMS analysis, 3 μL of the sample was injected into a Dionex Ultimate 3000 UPLC equipped with a Waters Xbridge BEH C18 2.5 μm column (100 × 3.0 mm Column XP) and PDA detector set to 210, 280, and 320 nm. Acetic acid (1% in water) was used as solvent A, and methanol was used as solvent B at a 0.5 mL/min flow rate. The total gradient program was set to 75 min. It involved programming 2% B to 5% B (10 min), 5% B to 20% B (50 min), 20% B to 50% (20 min), and 50% B to 2% (5 min). The method used for LCMS analysis was based on the method by McRae and Monreal.[80] The observed dimers and sucrose isomers were identified by MS/MS spectra using an in-house spectral library.

4.6. Catalyst Reusability Tests. Around 1.01 g of sugars, 0.05 g of catalyst, 1.00 g of [BMIM]Cl, and 3.5 mL (3.00 g) of MeTHF were mixed in a glass pressure tube and heated to 125 °C for 10 min while stirring at 800 rpm. After the reaction mixture was cooled to room temperature, the organic MeTHF phase was separated. Then, the carbon catalyst in the [BMIM]Cl phase was isolated by centrifugation and washed with acetone until a clear solution was observed. The isolated catalyst was vacuum-dried at 60 °C for 24 h. The dried catalyst was weighed, and the sugars-to-catalyst weight ratio of 20.2:1 was maintained in the reusability tests.

The elemental compositions of fresh and recovered catalysts were determined by using a Flash EA Organic Analyzer (Thermoscientific, US). Prior to analysis, samples were dried overnight at 45 °C in a vacuum oven. Thermogravimetric analysis was performed on fresh and spent catalysts by using a TA Instrument Q500 in air at 800 °C with a heating rate of 10 °C min^{-1}. The total organic carbon (TOC) contents present in both the fresh and spent catalysts IL medium were measured by a total organic carbon analyzer (Shimadzu TOC-V, Australia). Further, detailed characterization of the spent catalyst was conducted by using N_2 adsorption−desorption analysis, XRD, XPS, SEM, and Raman analysis.

The heterogeneity and the affinity of $-SO_3H$ groups onto the carbon were analyzed by the hot filtration method.[81] The method involved filtering the solid catalyst after reaction (1.01 g of sucrose, 0.05 g of catalyst, 1.00 g of [BMIM]Cl, and 3.5 mL (3.00 g) of MeTHF for 10 min at 125 °C) while the reaction mixture was hot. Afterward, fresh sucrose (1.01 g) was added to the filtrate, and the conversion to HMF was conducted for 10 min at 125 °C.

■ ASSOCIATED CONTENT

Supporting Information

The Supporting Information is available free of charge at https://pubs.acs.org/doi/10.1021/acsomega.3c05060.

Figure S1. Energy-dispersive X-ray spectroscopy (EDS) mapping of HSO3Cl catalyst, including SEM image (a), C element (b), O element (c), S element (d), and Cl element (e). Figure S2. (a) XPS wide spectrum, (b) C 1s high-resolution spectrum, (c) O 1s high-resolution spectrum, and (d) S 2p high-resolution spectrum of sulfonated carbon. Reproduced with permission from ref 1. Copyright 2021 Fuel. Figure S3. (a) N2 adsorption−desorption isotherm, (b) pore size distribution spectrum, (c) curve fitted XRD pattern corresponding to 002 and 100 planes, and (d) Raman spectrum of sulfonated carbon. Reproduced with permission from ref 1. Copyright 2021 Fuel. Figure S4. The effect of glucose wt % in glucose conversion vs HMF yield (1.01 g of substrate, 1.00 g of [BMIM]Cl, 0.05 g of catalyst, and 3.00 g of MeTHF; 125 °C; 10 min). Figure S5. Reaction intermediates formed in the dehydration of fructose to HMF. Reproduced with permission from ref 2. Copyright 2015 ACS publications. Figure S6. The *p*-TsOH carbon catalyst XPS (a) wide spectrum, (b) wide spectrum after the fourth run, (c) S 2p high-resolution spectrum, and (d) S 2p high-resolution spectrum after the fourth run. Figure S7. LCMS spectra of standard solutions (a) fructose, (b) glucose, and (c) sucrose and corresponding ESI(+)-MS spectra of (d) fructose, (e) glucose, and (f) sucrose. Figure S8. (a) LCMS spectrum (0.0−4.0 min) of fructose solution (20 wt %) and corresponding ESI(+)-MS spectra of peaks at (b) 1.06−1.11 min, (c) 1.14−1.21 min, and (d) 1.31−1.40 min observed in the production of HMF by the carbon catalyst at 125 °C in 10 min (sugars, 1.01 g; [BMIM]Cl, 1 g; catalyst, 0.05 g). Figure S9. (a) LCMS spectrum (0.0−4.25 min) of glucose solution (20 wt %) and corresponding ESI(+)-MS spectra of peaks at (b) 0.96−1.10 min and (c) 1.11−1.13 min observed in the production of HMF by the carbon catalyst at 125 °C in 10 min (sugars, 1.01 g; [BMIM]Cl, 1 g; catalyst, 0.05 g). Figure S10. (a) LCMS spectrum (0.0−4.23 min) of sucrose solution (20 wt %) and corresponding ESI(+)-MS spectra of peaks at (b) 0.97−1.12 min, (c) 1.13−1.21 min, and (d) 1.28−1.40 min observed in the production of HMF by the carbon catalyst at 125 °C in 10 min (sugars, 1.01 g; [BMIM]Cl, 1 g; catalyst, 0.05 g). Figure S11. (a) LCMS spectrum (0.0−4.12 min) of fructose/glucose (50/50) solution (20 wt %) and corresponding ESI(+)-MS spectra of peaks at (b) 0.97−1.11 min, (c) 1.14−1.23 min, and (d) 1.31−1.42

https://doi.org/10.1021/acsomega.3c05060
ACS Omega 2023, 8, 40442−40455

min observed in the production of HMF by the carbon catalyst at 125 °C in 10 min (sugars, 1.01 g; [BMIM]Cl, 1 g; catalyst, 0.05 g). Figure S12. Suggested molecular and fragmentation ion structures corresponding to the peaks observed in ESI(+)-MS spectra of sugars in the conversion to HMF by the carbon catalyst at 125 °C in 10 min (1.01 g of sugars, 1.00 g of [BMIM]Cl, and 0.05 g of catalyst). Figure S13. ESI(+)-MS spectrum corresponding to the m/z 145 signal observed in the LCMS spectrum (38.41−38.46 min) for the conversion of sucrose (20 wt %) to HMF using sulfonated catalyst at 125 °C in 10 min (sugars, 1,01 g; [BMIM]Cl, 1 g; catalyst, 0.05 g). Figure S14. HPLC spectra of (a) concentrated sucrose converted to HMF at 125 °C after 10 min and (b) diluted (4.54 wt %) fructose converted to HMF at different reaction times. Figure S15. TOC content of solution obtained from fresh and recovered catalysts. Table S1. Compositional analysis data of CGT. Table S2. Elemental analysis of sulfonated catalysts by chlorosulfonic acid and *p*-TsOH acid and their spent catalysts. Table S3. Assignments of peaks identified in MS chromatograms of concentrated sugar solution in positive ionization mode (PDF)

AUTHOR INFORMATION

Corresponding Author

Darryn W. Rackemann − *Centre for Agriculture and the Bioeconomy, Queensland University of Technology, Brisbane, Queensland 4001, Australia;* orcid.org/0000-0002-5055-6483; Email: d.rackemann@qut.edu.au

Authors

Athukoralalage Don K. Deshan − *Centre for Agriculture and the Bioeconomy, Queensland University of Technology, Brisbane, Queensland 4001, Australia*

Lalehvash Moghaddam − *Centre for Agriculture and the Bioeconomy, Queensland University of Technology, Brisbane, Queensland 4001, Australia;* orcid.org/0000-0003-2999-8700

Luqman Atanda − *Centre for Agriculture and the Bioeconomy, Queensland University of Technology, Brisbane, Queensland 4001, Australia;* orcid.org/0000-0002-9810-120X

Hongxia Wang − *School of Chemistry and Physics, Faculty of Science, Queensland University of Technology, Brisbane, Queensland 4001, Australia;* orcid.org/0000-0003-0146-5259

John P. Bartley − *School of Chemistry and Physics, Faculty of Science, Queensland University of Technology, Brisbane, Queensland 4001, Australia*

William O.S. Doherty − *Faculty of Science and Engineering, Southern Cross University, Lismore, New South Wales 2480, Australia; Doherty Consulting Services, Brisbane, Queensland 4116, Australia*

Complete contact information is available at: https://pubs.acs.org/10.1021/acsomega.3c05060

Author Contributions

The manuscript was written through contributions of all authors. All authors have given approval to the final version of the manuscript.

Funding

Funding source: Queensland University of Technology, Brisbane, Australia.

Notes

The authors declare no competing financial interest.

ACKNOWLEDGMENTS

The authors acknowledge the Centre for Agriculture and the Bioeconomy (CAB), Queensland University of Technology, Brisbane, Australia, for the support given. The authors would also like to acknowledge the QUT staff and the Central Analytical Research Facility (CARF) for their assistance in using analytical equipment.

ABBREVIATIONS

CGT, cotton gin trash; HMF, 5-hydroxymethyl furfural; FDCA, 2,5-furandicarboxylic acid; PEF, polyethylene furonate; PET, polyethylene terephthalate; DMSO, dimethylsulfoxide; LCMS, liquid chromatography−mass spectroscopy; SEM, scanning electron microscope; *p*-TsOH, *p*-toluenesulfonic acid; EDS, energy-dispersive spectroscopy; XPS, X-ray photoelectron spectroscopy; [BMIM]Cl, 1-butyl-3-methyl-imidazolium chloride; HPLC, high-performance liquid chromatography; XRD, X-ray powder diffraction; CPMAS, cross-polarization magic angle spinning; BET, Brunauer−Emmett−Teller

REFERENCES

(1) Abdilla-Santes, R. M.; Guo, W.; Bruijnincx, P. C.; Yue, J.; Deuss, P. J.; Heeres, H. High-yield 5-hydroxymethylfurfural synthesis from crude sugar beet juice in a biphasic microreactor. *ChemSusChem* **2019**, *12* (18), 4304.

(2) Hou, Q.; Qi, X.; Zhen, M.; Qian, H.; Nie, Y.; Bai, C.; Zhang, S.; Bai, X.; Ju, M. Biorefinery roadmap based on catalytic production and upgrading 5-hydroxymethylfurfural. *Green Chem.* **2021**, *23* (1), 119−231.

(3) Fulignati, S.; Antonetti, C.; Wilbers, E.; Licursi, D.; Heeres, H. J.; Raspolli Galletti, A. M. Tunable HMF hydrogenation to furan diols in a flow reactor using Ru/C as catalyst. *J. Ind. Eng. Chem.* **2021**, *100* (390), e1−390.e9.

(4) Pal, P.; Saravanamurugan, S. Recent advances in the development of 5-hydroxymethylfurfural oxidation with base (nonprecious)-metal-containing catalysts. *ChemSusChem* **2019**, *12* (1), 145−163.

(5) Hu, H.; Xue, T.; Zhang, Z.; Gan, J.; Chen, L.; Zhang, J.; Qu, F.; Cai, W.; Wang, L. Direct conversion of 5-hydroxymethylfurfural to furanic diether by copper-loaded hierarchically structured ZSM-5 catalyst in a fixed-bed reactor. *ChemCatChem* **2021**, *13* (15), 3461−3469.

(6) Guo, D.; Lai, J.; Cheng, F.; Zhao, W.; Chen, H.; Li, H.; Liu, X.; Yin, D.; Yu, N. Titanium silicalite-1 supported bimetallic catalysts for selective hydrogenolysis of 5-hydroxymethylfurfural to biofuel 2, 5-dimethylfuran. *Chem. Eng. J. Adv.* **2021**, *5*, No. 100081.

(7) Zhou, J.; Xia, Z.; Huang, T.; Yan, P.; Xu, W.; Xu, Z.; Wang, J.; Zhang, Z. C. An ionic liquid−organics−water ternary biphasic system enhances the 5-hydroxymethylfurfural yield in catalytic conversion of glucose at high concentrations. *Green Chem.* **2015**, *17* (8), 4206−4216.

(8) Hou, Q.; Zhen, M.; Liu, L.; Chen, Y.; Huang, F.; Zhang, S.; Li, W.; Ju, M. Tin phosphate as a heterogeneous catalyst for efficient dehydration of glucose into 5-hydroxymethylfurfural in ionic liquid. *Applied Catalysis B: Environmental* **2018**, *224*, 183−193.

(9) Herbst, A.; Janiak, C. Selective glucose conversion to 5-hydroxymethylfurfural (5-HMF) instead of levulinic acid with MIL-101Cr MOF-derivatives. *New J. Chem.* **2016**, *40* (9), 7958−7967.

(10) Ranu, B. C.; Dey, S. S.; Hajra, A.; Ramsden, C. A. Solvent-free, catalyst-free Michael-type addition of amines to electron-deficient alkenes. *Arkivoc* **2002**, *2002*, 76.
(11) Howard, J.; Rackemann, D. W.; Bartley, J. P.; Samori, C.; Doherty, W. O. S. Conversion of sugar cane molasses to 5-hydroxymethylfurfural using molasses and bagasse-derived catalysts. *ACS Sustainable Chem. Eng.* **2018**, *6* (4), 4531−4538.
(12) Deshan, A. D. K.; Forero, J. J.; Bartley, J. P.; Marasinghege, C.; Tuiatua, K.; Beltramini, J.; Doherty, W. O. S. Structural features of cotton gin trash derived carbon material as a catalyst for the dehydration of fructose to 5-hydroxymethylfurfural. *Fuel* **2021**, *306*, No. 121670.
(13) Cao, L.; Yu, I. K. M.; Chen, S. S.; Tsang, D. C. W.; Wang, L.; Xiong, X.; Zhang, S.; Ok, Y. S.; Kwon, E. E.; Song, H.; Poon, C. S. Production of 5-hydroxymethylfurfural from starch-rich food waste catalyzed by sulfonated biochar. *Bioresour. Technol.* **2018**, *252*, 76−82.
(14) Xiong, X.; Yu, I. K. M.; Chen, S. S.; Tsang, D. C. W.; Cao, L.; Song, H.; Kwon, E. E.; Ok, Y. S.; Zhang, S.; Poon, C. S. Sulfonated biochar as acid catalyst for sugar hydrolysis and dehydration. *Catal. Today* **2018**, *314*, 52−61.
(15) Shen, Z.; Yu, X.; Chen, J. Production of 5-hydroxymethylfurfural from fructose catalyzed by sulfonated bamboo-derived carbon prepared by simultaneous carbonization and sulfonation. *BioResources* **2016**, *11*, 3094−3109.
(16) Jia, S.; Liu, K.; Xu, Z.; Yan, P.; Xu, W.; Liu, X.; Zhang, Z. C. Reaction media dominated product selectivity in the isomerization of glucose by chromium trichloride: From aqueous to non-aqueous systems. *Catal. Today* **2014**, *234*, 83−90.
(17) Barbosa, S. L.; de, S.; Freitas, M.; dos Santos, W. T. P.; Nelson, D. L.; Klein, S. I.; Clososki, G. C.; Caires, F. J.; Baroni, A. C. M.; Wentz, A. P. Dehydration of d-fructose to 5-hydroxymethyl-2-furfural in DMSO using a hydrophilic sulfonated silica catalyst in a process promoted by microwave irradiation. *Sci. Rep.* **2021**, *11* (1), 1919.
(18) Zhang, Z. C. Catalytic transformation of carbohydrates and lignin in ionic liquids. *Wiley Interdiscip. Rev.: Energy Environ.* **2013**, *2* (6), 655−672.
(19) Bai, C.; Hou, Q.; Bai, X.; Nie, Y.; Qian, H.; Zhen, M.; Ju, M. Conversion of glucose to 5-hydroxymethylfurfural at high substrate loading: Effect of catalyst and solvent on the stability of 5-hydroxymethylfurfural. *Energy Fuels* **2020**, *34* (12), 16240−16249.
(20) Cheng, T.-Y.; Chao, P.-Y.; Huang, Y.-H.; Li, C.-C.; Hsu, H.-Y.; Chao, Y.-S.; Tsai, T.-C. Catalysis of ordered nanoporous materials for fructose dehydration through difructose anhydride intermediate. *Microporous Mesoporous Mater.* **2016**, *233*, 148−153.
(21) Plácido, J.; Imam, T.; Capareda, S., Bioethanol production from cotton gin trash: A new process route. In *Beltwide Cotton Conference*; Orlando FL, 2012; pp 3−6.
(22) Yasuda, S.; Hamaguchi, E.; Asano, K. Ready chemical conversion of acid hydrolysis lignin into water-soluble lignosulfonate III: Successive treatment of acid hydrolysis lignin and a lignin model compound by phenolation and arylsulfonation. *Journal of Wood Science* **1999**, *45* (3), 245−249.
(23) Wu, B.; Lin, X.; Ge, L.; Wu, L.; Xu, T. A novel route for preparing highly proton conductive membrane materials with metal-organic frameworks. *Chem. Commun.* **2012**, *49*, 143−145, DOI: 10.1039/C2CC37045J.
(24) Sata, T.; Izuo, R.; Takata, K. Modification of the transport properties of ion exchange membranes. IX. Layer formation on a cation exchange membrane by acid-amide bonding, and transport properties of the resulting membrane. *Science* **1989**, *45* (3), 197−208.
(25) Painter, P.; Starsinic, M.; Coleman, M. Determination of functional groups in coal by Fourier transform interferometry. *Fourier Transform Infrared Spectrosc.* **2012**, *4*, 169−240.
(26) Wang, S.-H.; Griffiths, P. R. Resolution enhancement of diffuse reflectance i.r. spectra of coals by Fourier self-deconvolution: 1. C-H stretching and bending modes. *Fuel* **1985**, *64* (2), 229−236.
(27) Hara, M. Biomass conversion by a solid acid catalyst. *Energy Environ. Sci.* **2010**, *3* (5), 601−607.
(28) Nakajima, K.; Hara, M. Amorphous carbon with SO3H groups as a solid Brønsted acid catalyst. *ACS Catal.* **2012**, *2* (7), 1296−1304.
(29) Konwar, L. J.; Mäki-Arvela, P.; Salminen, E.; Kumar, N.; Thakur, A. J.; Mikkola, J.-P.; Deka, D. Towards carbon efficient biorefining: Multifunctional mesoporous solid acids obtained from biodiesel production wastes for biomass conversion. *Appl. Catal. B* **2015**, *176−177*, 20−35.
(30) Zhao, J.; Zhou, C.; He, C.; Dai, Y.; Jia, X.; Yang, Y. Efficient dehydration of fructose to 5-hydroxymethylfurfural over sulfonated carbon sphere solid acid catalysts. *Catal. Today* **2016**, *264*, 123−130.
(31) Chen, C.; Xu, G.; Wei, X.; Yang, L. A macroscopic three-dimensional tetrapod-separated graphene-like oxygenated N-doped carbon nanosheet architecture for use in supercapacitors. *J. Mater. Chem. A* **2016**, *4* (25), 9900−9909.
(32) Okamura, M.; Takagaki, A.; Toda, M.; Kondo, J. N.; Domen, K.; Tatsumi, T.; Hara, M.; Hayashi, S. Acid-catalyzed reactions on flexible polycyclic aromatic carbon in amorphous carbon. *Chem. Mater.* **2006**, *18* (13), 3039−3045.
(33) Luan, S.; Li, W.; Guo, Z.; Li, W.; Hou, X.; Song, Y.; Wang, R.; Wang, Q. Synthesis of ordered hierarchically mesoporous/microporous carbon materials via compressed CO2 for fructose-to-HMF transformation. *Green Energy Environ.* **2021**, *7*, 1033−1044, DOI: 10.1016/j.gee.2021.01.005.
(34) Dong, K.; Zhang, J.; Luo, W.; Su, L.; Huang, Z. Catalytic conversion of carbohydrates into 5-hydroxymethyl furfural over sulfonated hyper-cross-linked polymer in DMSO. *Chem. Eng. J.* **2018**, *334*, 1055−1064.
(35) Wang, C.; Gui, X.; Yun, Z. Esterification of lauric and oleic acids with methanol over oxidized and sulfonated activated carbon catalyst. *React. Kinet., Mech. Catal.* **2014**, *113* (1), 211−223.
(36) Sayigh, A. *Renewable energy in the service of mankind Vol I: Selected topics from the world renewable energy congress WREC 2014*; Springer Cham: Brighton, 2015; Vol. *I*, DOI: 10.1007/978-3-319-17777-9.
(37) de Clippel, F.; Dusselier, M.; Van de Vyver, S.; Peng, L.; Jacobs, P. A.; Sels, B. F. Tailoring nanohybrids and nanocomposites for catalytic applications. *Green Chem.* **2013**, *15* (6), 1398−1430.
(38) Al-Amsyar, S. M. Sulfonated-silica/carbon composites from rice husk as heterogeneous catalysts in fructose conversion: The effect of controlling carbonization temperature of rice husk on its physicochemical properties and catalytic activities. *Microporous Mesoporous Mater.* **2022**, *336*, No. 111896.
(39) Agrawal, A.; Kaushik, N.; Biswas, S. Derivatives and applications of lignin-An insight. *SciTech J.* **2014**, *1* (7), 30−36.
(40) Li, H.; Yang, S.; Saravanamurugan, S.; Riisager, A. Glucose isomerization by enzymes and chemo-catalysts: Status and current advances. *ACS Catal.* **2017**, *7* (4), 3010−3029.
(41) Gao, X.; Zhong, H.; Yao, G.; Guo, W.; Jin, F. Hydrothermal conversion of glucose into organic acids with bentonite as a solid-base catalyst. *Catal. Today* **2016**, *274*, 49−54.
(42) Zhang, H.; Li, N.; Pan, X.; Wu, S.; Xie, J. Oxidative conversion of glucose to gluconic acid by iron(iii) chloride in water under mild conditions. *Green Chem.* **2016**, *18* (8), 2308−2312.
(43) Guo, W.; Heeres, H. J.; Yue, J. Continuous synthesis of 5-hydroxymethylfurfural from glucose using a combination of AlCl3 and HCl as catalyst in a biphasic slug flow capillary microreactor. *Chem. Eng. J.* **2020**, *381*, No. 122754.
(44) Hou, Q.; Li, W.; Zhen, M.; Liu, L.; Chen, Y.; Yang, Q.; Huang, F.; Zhang, S.; Ju, M. An ionic liquid-organic solvent biphasic system for efficient production of 5-hydroxymethylfurfural from carbohydrates at high concentrations. *RSC Adv.* **2017**, *7* (75), 47288−47296.
(45) Dutta, S.; De, S.; Saha, B. Advances in biomass transformation to 5-hydroxymethylfurfural and mechanistic aspects. *Biomass Bioenergy* **2013**, *55*, 355−369.
(46) Zhang, Y.; Pidko, E. A.; Hensen, E. J. M. Molecular aspects of glucose dehydration by chromium chlorides in ionic liquids. *Chem.—Eur. J.* **2011**, *17* (19), 5281−5288.
(47) Boronat, M.; Corma, A.; Renz, M. Mechanism of the Meerwein−Ponndorf−Verley−Oppenauer (MPVO) Redox Equili-

https://doi.org/10.1021/acsomega.3c05060
ACS Omega 2023, 8, 40442−40455

brium on Sn− and Zr−Beta Zeolite Catalysts. *J. Phys. Chem. B* **2006**, *110* (42), 21168−21174.
(48) Ravasco, J. M. J. M.; Coelho, J. A. S.; Simeonov, S. P.; Afonso, C. A. M. Bifunctional Cr3+ modified ion exchange resins as efficient reusable catalysts for the production and isolation of 5-hydroxymethylfurfural from glucose. *RSC Adv.* **2017**, *7* (13), 7555−7559.
(49) Qi, X.; Liu, N.; Lian, Y. Carbonaceous microspheres prepared by hydrothermal carbonization of glucose for direct use in catalytic dehydration of fructose. *RSC Adv.* **2015**, *5* (23), 17526−17531.
(50) Qi, X.; Guo, H.; Li, L.; Smith, R. L., Jr. Acid-catalyzed dehydration of fructose into 5-hydroxymethylfurfural by cellulose-derived amorphous carbon. *ChemSusChem* **2012**, *5* (11), 2215−2220.
(51) Hu, L.; Zhao, G.; Tang, X.; Wu, Z.; Xu, J.; Lin, L.; Liu, S. Catalytic conversion of carbohydrates into 5-hydroxymethylfurfural over cellulose-derived carbonaceous catalyst in ionic liquid. *Bioresour. Technol.* **2013**, *148*, 501−507.
(52) Li, X.; Wang, Y.; Xie, X.; Huang, C.; Yang, S. Dehydration of fructose, sucrose and inulin to 5-hydroxymethylfurfural over yeast-derived carbonaceous microspheres at low temperatures. *RSC Adv.* **2019**, *9* (16), 9041−9048.
(53) Xie, H.; Zhao, Z. K.; Wang, Q. Catalytic conversion of inulin and fructose into 5-hydroxymethylfurfural by lignosulfonic acid in ionic liquids. *ChemSusChem* **2012**, *5* (5), 901−905.
(54) Guo, F.; Fang, Z.; Zhou, T.-J. Conversion of fructose and glucose into 5-hydroxymethylfurfural with lignin-derived carbonaceous catalyst under microwave irradiation in dimethyl sulfoxide-ionic liquid mixtures. *Bioresour. Technol.* **2012**, *112*, 313−318.
(55) Shen, F.; Smith, R. L., Jr; Li, L.; Yan, L.; Qi, X. Eco-friendly method for efficient conversion of cellulose into levulinic acid in pure water with cellulase-mimetic solid acid catalyst. *ACS Sustainable Chem. Eng.* **2017**, *5* (3), 2421−2427.
(56) Shuai, L.; Pan, X. Hydrolysis of cellulose by cellulase-mimetic solid catalyst. *Energy Environ. Sci.* **2012**, *5* (5), 6889−6894.
(57) Yan, L.; Liu, N.; Wang, Y.; Machida, H.; Qi, X. Production of 5-hydroxymethylfurfural from corn stalk catalyzed by corn stalk-derived carbonaceous solid acid catalyst. *Bioresour. Technol.* **2014**, *173*, 462−466.
(58) Kitano, M.; Yamaguchi, D.; Suganuma, S.; Nakajima, K.; Kato, H.; Hayashi, S.; Hara, M. Adsorption-enhanced hydrolysis of β-1,4-glucan on graphene-based amorphous carbon bearing SO_3H, COOH, and OH groups. *Langmuir* **2009**, *25* (9), 5068−5075.
(59) Suganuma, S.; Nakajima, K.; Kitano, M.; Yamaguchi, D.; Kato, H.; Hayashi, S.; Hara, M. Hydrolysis of cellulose by amorphous carbon bearing SO_3H, COOH, and OH groups. *J. Am. Chem. Soc.* **2008**, *130* (38), 12787−12793.
(60) Tian, Y.; Zhang, R.; Zhao, W.; Wen, S.; Xiang, Y.; Liu, X. A new sulfonic acid-functionalized organic polymer catalyst for the synthesis of biomass-derived alkyl levulinates. *Catal. Lett.* **2020**, *150* (12), 3553−3560.
(61) Binder, J. B.; Raines, R. T. Simple chemical transformation of lignocellulosic biomass into furans for fuels and chemicals. *J. Am. Chem. Soc.* **2009**, *131* (5), 1979−1985.
(62) Zhao, H.; Holladay, J. E.; Brown, H.; Zhang, Z. C. Metal chlorides in ionic liquid solvents convert sugars to 5-hydroxymethylfurfural. *Science* **2007**, *316* (5831), 1597−1600.
(63) Hou, Q.; Zhen, M.; Li, W.; Liu, L.; Liu, J.; Zhang, S.; Nie, Y.; Bai, C.; Bai, X.; Ju, M. Efficient catalytic conversion of glucose into 5-hydroxymethylfurfural by aluminum oxide in ionic liquid. *Appl. Catal. B* **2019**, *253*, 1−10.
(64) Thavarajah, P.; Low, N. H. Isolation and identification of select oligosaccharides from commercially produced total invert sugar with a proposed mechanism for their formation. *J. Agric. Food Chem.* **2006**, *54* (7), 2754−2760.
(65) Tan-Soetedjo, J. N. M.; van de Bovenkamp, H. H.; Abdilla, R. M.; Rasrendra, C. B.; van Ginkel, J.; Heeres, H. J. Experimental and kinetic modeling studies on the conversion of sucrose to levulinic acid and 5-hydroxymethylfurfural using sulfuric acid in water. *Ind. Eng. Chem. Res.* **2017**, *56* (45), 13228−13239.
(66) Pilath, H. M.; Nimlos, M. R.; Mittal, A.; Himmel, M. E.; Johnson, D. K. Glucose reversion reaction kinetics. *J. Agric. Food Chem.* **2010**, *58* (10), 6131−6140.
(67) Thompson, J.; Robrish, S. A.; Immel, S.; Lichtenthaler, F. W.; Hall, B. G., II; Pikis, A. Metabolism of sucrose and its five linkage-isomeric α-d-glucosyl-d-fructoses by Klebsiella pneumoniae: Participation and properties of sucrose-6-phosphate hydrolase and phospho-α-glucosidase. *J. Biol. Chem.* **2001**, *276* (40), 37415−37425.
(68) Huang, Y.; Chao, P.-Y.; Cheng, T.-Y.; Ho, Y.; Lin, C.-T.; Hsu, H.-Y.; Wong, J.-J.; Tsai, T.-C. Design of sulfonated mesoporous silica catalyst for fructose dehydration guided by difructose anhydride intermediate incorporated reaction network. *Chem. Eng. J.* **2016**, *283*, 778−788.
(69) Crisci, A. J.; Tucker, M. H.; Lee, M.-Y.; Jang, S. G.; Dumesic, J. A.; Scott, S. L. Acid-functionalized SBA-15-type silica catalysts for carbohydrate dehydration. *ACS Catal.* **2011**, *1* (7), 719−728.
(70) Akien, G. R.; Qi, L.; Horváth, I. T. Molecular mapping of the acid catalysed dehydration of fructose. *Chem. Commun.* **2012**, *48* (47), 5850−5852.
(71) Zhang, J.; Yu, X.; Zou, F.; Zhong, Y.; Du, N.; Huang, X. Room-temperature ionic liquid system converting fructose into 5-hydroxymethylfurfural in high efficiency. *ACS Sustainable Chem. Eng.* **2015**, *3* (12), 3338−3345.
(72) Huo, J.; Pham, H. N.; Cheng, Y.; Lin, H.-H.; Roling, L. T.; Datye, A. K.; Shanks, B. H. Deactivation and regeneration of carbon supported Pt and Ru catalysts in aqueous phase hydrogenation of 2-pentanone. *Cat. Sci. Tech* **2020**, *10* (9), 3047−3056.
(73) Sluiter, A.; Hames, B.; Ruiz, R.; Scarlata, C.; Sluiter, J.; Templeton, D.; Crocker, D. Determination of structural carbohydrates and lignin in biomass. *Laboratory Analytical Procedure* **2008**, *1617*, 1−16.
(74) Chhabra, T.; Bahuguna, A.; Dhankhar, S. S.; Nagaraja, C. M.; Krishnan, V. Sulfonated graphitic carbon nitride as a highly selective and efficient heterogeneous catalyst for the conversion of biomass-derived saccharides to 5-hydroxymethylfurfural in green solvents. *Green Chem.* **2019**, *21* (21), 6012−6026.
(75) Dechakhumwat, S.; Hongmanorom, P.; Thunyaratchatanon, C.; Smith, S. M.; Boonyuen, S.; Luengnaruemitchai, A. Catalytic activity of heterogeneous acid catalysts derived from corncob in the esterification of oleic acid with methanol. *Renewable Energy* **2020**, *148*, 897−906.
(76) Meng, J.; Li, S.; Niu, J. Crystallite structure characteristics and its influence on methane adsorption for different rank coals. *ACS Omega* **2019**, *4* (24), 20762−20772.
(77) Boehm, H. P. Some aspects of the surface chemistry of carbon blacks and other carbons. *Carbon* **1994**, *32* (5), 759−769.
(78) Yu, S.-B.; Zang, H.-J.; Yang, X.-L.; Zhang, M.-C.; Xie, R.-R.; Yu, P.-F. Highly efficient preparation of 5-hydroxymethylfurfural from sucrose using ionic liquids and heteropolyacid catalysts in dimethyl sulfoxide−water mixed solvent. *Chin. Chem. Lett.* **2017**, *28* (7), 1479−1484.
(79) Li, H.; Yang, S. Catalytic transformation of fructose and sucrose to HMF with proline-derived ionic liquids under mild conditions. *Int. J. Chem. Eng.* **2014**, *2014*, No. 978708.
(80) McRae, G.; Monreal, C. M. LC-MS/MS quantitative analysis of reducing carbohydrates in soil solutions extracted from crop rhizospheres. *Anal. Bioanal. Chem.* **2011**, *400*, 2205−2215.
(81) Sun, Q.; Wang, S.; Aguila, B.; Meng, X.; Ma, S.; Xiao, F.-S. Creating solvation environments in heterogeneous catalysts for efficient biomass conversion. *Nat. Commun.* **2018**, *9* (1), 3236.

https://doi.org/10.1021/acsomega.3c05060
ACS Omega 2023, 8, 40442−40455